ACS OMEGA

Open Access

http://pubs.acs.org/journal/acsodf

Article

Effect of Fatty Acid Unsaturation on the Intermolecular Weak Interaction at the Low-Rank Coal−Water Interface: Density Functional Theory Calculations and Experimental Study

Zechen Liu,* Xianshu Dong,* Yinfei Liao, Yuping Fan, and Yijun Cao

Cite This: *ACS Omega* 2024, 9, 21071−21081

Read Online

ACCESS | Metrics & More | Article Recommendations

ABSTRACT: The study on the effect of fatty acid saturation on low-rank coal (LRC) flotation is still limited. In this investigation, density functional theory (DFT) combined with Zeta potential and Fourier transform infrared spectroscopy (FTIR) was used to study the mechanism of intermolecular weak interaction at the LRC−water interface of fatty acids (decanoic acid (DA), undecylenic acid (UA), and phenyl propionic acid (PA)) with different saturations and different dodecane (D) composition hydrocarbon oil−fatty acid mixed collectors (D-DA, D-UA, D-PA). The findings demonstrated that the hydrogen bond interaction and electrostatic interaction between the UA/PA with unsaturated bonded carbon chains and the LRC molecular fragments/water molecules were stronger than DA without a saturated bond carbon chain, and UA/PA strengthened its interaction with water molecules on the whole, even PA molecules would preferentially interact with water molecules. The unsaturated bond had a minimal impact on the adsorption of the LRC hydrophobic site, and the strength of the hydrogen bond between the mixed collector and LRC is D-DA > D-UA > D-PA. In the actual flotation process, the strong hydrogen bonding and electrostatic interaction between UA/PA and water molecules weaken the collection performance of the mixed collector D-UA/D-PA for LRC, which also confirmed the research results of DFT, FTIR, and Zeta.

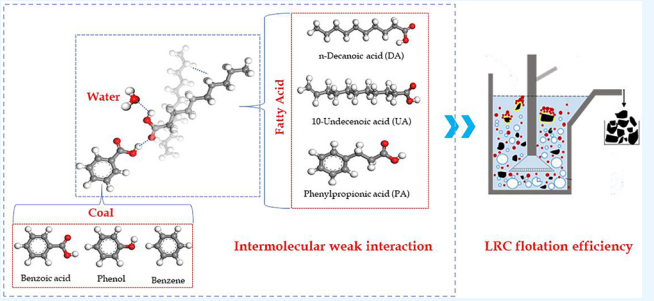

1. INTRODUCTION

Flotation is an effective means to enhance the separation of low-rank coal (LRC), but the bottleneck problems of LRC are low flotation efficiency and large pharmaceutical consumption caused by poor surface hydrophobicity.[1−3] The mixed collector consisting of a polar solid affinity group and a nonpolar hydrocarbon group can improve the flotation efficiency of the LRC well.[4−6] Among them, the application of a hydrocarbon oil−fatty acid mixed collector is increasing gradually. Hydrocarbon oil can effectively increase the surface hydrophobicity of coal particles and the strength of coal particles and bubble adhesion, and the carboxyl group in fatty acids can act on a variety of functional groups containing oxygen on the LRC surface.[7−9] Liu et al.[10] obtained a better harvesting effect for LRC by using the mixed collector composed of dodecane and *n*-valeric acid. Li et al.[11] used shale oil to greatly improve the flotation efficiency of oxidized coal, mainly because unsaturated fatty acids and more long-chain hydrocarbons existed in shale oil, which led to stronger hydrophobicity of coal surface and promoted the adhesion of bubble particles. Liao et al.[12] used a complex collector composed of dodecane and oleic acid to enhance the LRC surface's hydrophobicity and promote the dynamics of bubble interaction with the LRC surface. For the hydrocarbon oil−fatty acid mixed collector, it can be found that there are both saturated and unsaturated fatty acids in the choice of fatty acids. In some mineral flotation, researchers have found that mixed fatty acids with a higher proportion of unsaturated fatty acids can enhance flotation.[13,14] However, research on the mechanism by which fatty acid saturation affects LRC flotation is still limited.

In the solid−liquid interface system, when collector molecules adsorb on the LRC surface, there are many weak intermolecular interactions between collector molecules, water molecules, and the LRC surface, mainly including hydrogen bond, van der Waals force, electrostatic interaction caused by dipole or charge, and hydrophilic/hydrophobic interaction.[15−17] At the LRC−water interface, the synergy and competition of these interaction forces largely determine the adsorption effect of mixed collector molecules and ultimately affect the LRC flotation efficiency. Density functional theory (DFT) is a reliable and effective technique for the study of interface interaction.[18,19] Many

Received: January 17, 2024
Revised: February 25, 2024
Accepted: April 19, 2024
Published: April 30, 2024

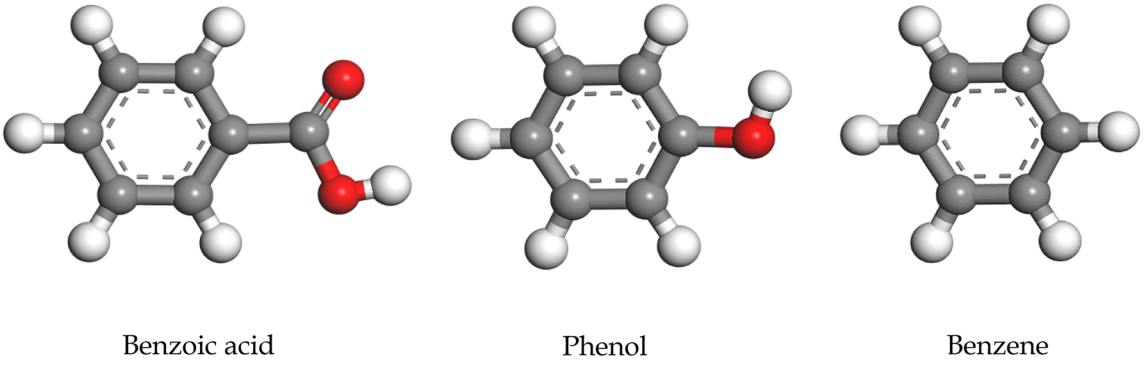

Figure 1. Molecular fragment structure of a typical low-rank coal.

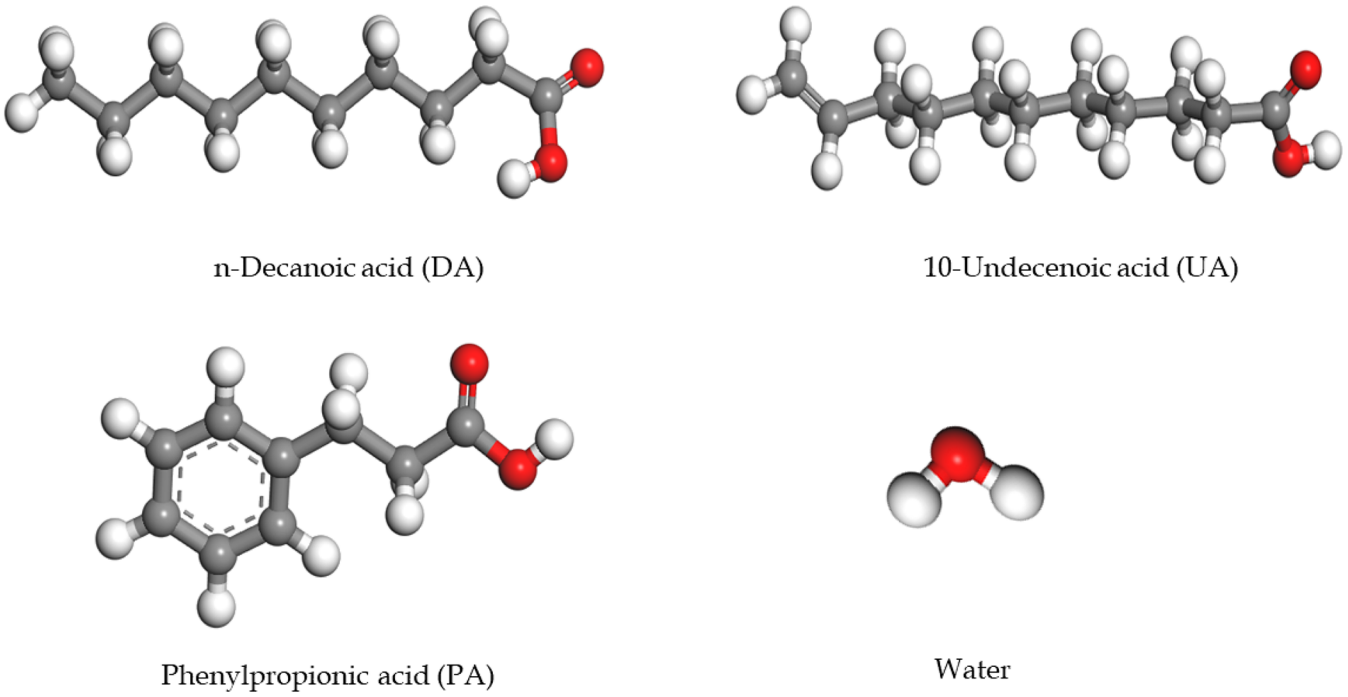

Figure 2. Fatty acid molecular models with different saturations and water molecular model.

scholars used DFT to calculate the charge transfer, state density, interaction distance, and energy between reagents and minerals to characterize the interaction between minerals and reagents.[20−22] Liu et al.[23] simulated the interaction of the sphalerite surface with ethyl xanthate (EX) and copper by utilizing the DFT method. The analysis of state density showed that the energy level difference between the bonded S 3p orbital and the Zn 3d orbital on the sphalerite surface led to the weak adsorption of EX on the unactivated sphalerite surface. Li et al.[24] explained how the surfactant lauryl polyoxyethylene ether ($C_{12}EO$) binds to the molecules on the LRC surface through DFT calculation. However, the comprehension of the weak interactions of mixed collector molecules at the LRC−water interface is not well understood, and the influence mechanism of fatty acid saturation on the weak interaction between molecules at the interface of the hydrocarbon oil−fatty acid mixed collector is worthy of further study.

Therefore, this work mainly studied the weak molecular interaction between the mixed collector composed of fatty acids and hydrocarbon oil with different saturations at the LRC−water interface through DFT simulation calculation and experiments and clarified the influence mechanism of fatty acids with different saturations on the mixed collector's adsorption at the LRC−water interface. The analysis and calculation of interface weak interactions by DFT gave theoretical backing for the design and development of mixed collectors.

2. MATERIALS AND EXPERIMENTAL METHODS

2.1. Materials. To examine the LRC, the long-flame coal from the Daliuta Coal Mine owned by the Shendong Group served as a representative. The samples were mainly raw coal and lump-cleaned coal. The ultralow ash coal with an ash content of 2.38% was prepared by processing the cleaned coal.[25,26] The obtained ultralow ash coal was ground into powder by a ball mill as a low-rank pure coal sample to research the LRC-collector interaction mechanism. The raw coal and some pure coal samples were obtained by a 0.5 mm sample screen for the macro flotation of −0.5 mm powder samples.

This work mainly studied the influence mechanism of fatty acids with different saturations on the mixed collector at the LRC−water interface. Therefore, when preparing the mixed collector, the hydrocarbon oil was dodecane (D), the saturation of fatty acids was changed, and three fatty acids (decanoic acid

https://doi.org/10.1021/acsomega.4c00572
ACS Omega 2024, 9, 21071−21081

(DA), 10-undecylenic acid (UA), and phenyl propionic acid (PA)) with carbon atomic numbers similar to those of dodecane were selected. Three kinds of hydrocarbon oil−fatty acid mixed collector, D-DA, D-UA, and D-PA, with different saturations were prepared by fixing the mass ratio of dodecane to fatty acid as 4:1.[27]

2.2. DFT Calculations. *2.2.1. Models.* The interaction between different kinds of carboxylic acid−hydrocarbon oil mixed collectors, LRC, and water was studied by using the DFT calculation method. Because hydrocarbon oil in the mixed collector is fixed to dodecane, the DFT calculation mainly studied the interaction between different types of carboxylic acid and LRC/water. Considering the computational power and cost of quantum chemistry, three LRC molecular fragments (benzoic acid, phenol, and benzene) with representative different polarities were selected for LRC,[28−30] as shown in Figure 1. The models of carboxylic acid molecules with different saturations and water molecules are shown in Figure 2.

2.2.2. Computational Method. The DFT calculation was completed by the CASTEP module, and the initial adsorption site was determined by the Sorption module. First, the CASTEP module was used to calculate the DFT for all individual molecules (each carboxylic acid molecule, LRC molecule fragment, and water molecule), and each molecule was in a 15 × 15 × 15 $Å^3$ cubic cell. In the process of DFT calculation, generalized gradient approximation (GGA)[31] jointly proposed by Perdew−Burke−Ernzerhof (PBE) was adopted for the exchange−correlation function, and dispersion force correction was carried out. 400 eV was changed as the cutoff energy, the core electron and the strong Coulomb potential were replaced by the ultrasoft pseudopotential wave function, and the atomic position was optimized by the Broyden−Fletcher−Goldfarb−Shanno (BFGS)[32] minimization algorithm and the K-point setting (1 × 1 × 1) of a single point in Gamma. Other geometric optimization parameters were set as follows: the energy convergence threshold was 2.0×10^{-5} eV/atom, the highest stress convergence threshold was 0.1 GPa, maximum convergence thresholds for force and displacement were 0.05 eV/Å and 0.002 Å, and the SCF (self-consistent field) convergence threshold was 2.0×10^{-6} eV/atom. Second, the Monte Carlo simulation of the Locate task in the Sorption module[33,34] was used to determine the priority adsorption sites between each carboxylic acid molecule with optimized structure and three LRC molecular fragments or water molecules, respectively. The COMPASS force field,[35,36] which was applied to organic molecules, inorganic molecules, and polymers, was used for the Monte Carlo simulation. The cycles were 15 times, and each cycle step was 10^5 steps. The Ewald group summation method was used to compute the electrostatic interaction, and the calculation accuracy was 0.0001 kcal/mol. The van der Waals interaction with a truncation distance of 15.5 Å was calculated using the Atom-based summation approach. A 40 Å thick vacuum plate was set to rid the *Z* axis of the influence of periodic boundary conditions. Finally, the DFT calculation was performed to further improve the adsorption model based on the preferred adsorption model that was determined by Monte Carlo calculation, and the optimization parameters were specified as previously mentioned.

2.3. Fourier Transform Infrared Spectroscopy (FTIR) Experiments. Three samples of the same fraction of pure coal (30 g per sample) were added to three samples of 500 mL of distilled water and formed a coal slurry after being agitated with a magnetic agitator for 3 min. Then three kinds of mixed collectors, D-DA, D-UA, and D-PA, containing different carboxylic acid types were added to the three samples of coal slurry in sequence (only one mixed collector was added to each coal slurry). The reagent was used at a dosage of 3 kg/t and continued to stir for 3 min. After the stirring, the three coal slurries treated with different kinds of mixed collectors were filtered before being dried at 40 °C in a vacuum oven. Both the mixed-collector-treated coal samples and the pure coal samples were evaluated using FTIR technology. The process of FTIR testing was to mix and press different coal samples at a mass ratio of 1:150 with potassium bromide and obtain the test spectra with a wavenumber of 400−4000 cm^{-1} and a spectral resolution of 2 cm^{-1}.[37,38]

2.4. Zeta Potential. Zeta potential analysis of LRC samples treated with different mixed collectors was measured and analyzed by Zeta Plus equipment. Four samples of the same fraction of pure coal (0.5 g per sample) were added to four samples of 50 mL of distilled water, and the mixture was agitated for 15 min with a magnetic agitator so that the coal samples were fully dispersed to form a suspension with a mass concentration of 1%. Three suspensions were given three different types of mixed collectors, each of which contained a different fatty acid (only one mixed collector was added to each suspension). The dosage of the reagent was 3 kg/t, and no reagent was added to the remaining suspension for the blank control test. All suspensions were allowed to stand for 24 h, and 4 doses of upper suspensions were drawn and inserted into the electrophoresis tank using a clean syringe. Based on the electrophoresis instrument's measuring process, under the conditions of a naturally occurring pH, the dynamic potential of pure coal samples adsorbed with various types of mixed fatty acids was studied. Each group of suspensions was measured five times, and the ultimate potential value of each sample was calculated by taking the average value.

2.5. Flotation Experiments. LRC flotation experiments were conducted using a 0.5L XFD single-cell flotation machine with a flotation pulp concentration of 60 g/L (that is, the LRC quality was 30 g). First, the coal used for flotation was a pure coal sample, and the collection performance of LRC with different saturations of hydrocarbon oil−fatty acid mixed collector was mainly investigated. The addition amounts of each collector in the flotation process were 0.3, 0.6, 1, 2, 3, 4, and 5 kg/t, respectively, and each time 2-octanol was employed as the frother, 0.3 kg/t was added. In the flotation process, the machine impeller speed was 1800 r/min, and the aeration was 0.25 m^3/h. After mixing for 3 min, the mixed collector was added and stirred for 3 min. After the frother was added for 30 s, the intake valve was opened, and 3 min were spent collecting the flotation clean coal. After flotation, the flotation clean coal yield was calculated after the collected coal samples had been filtered, dried, and weighed.

Then actual coal sample flotation was carried out. According to the flotation effect of the pure coal sample, the appropriate mixed collector addition system was selected. The dosage of other flotation agents, pulp concentration, and parameters were the same as the flotation settings of the above pure coal sample, and the effects of different kinds of mixed collectors in the actual LRC flotation were explored. After the flotation, the ash content of samples was obtained by burning the cleaned coal and the tailings, respectively, in the Muffle furnace. Ash content and the combustible matter recovery (Formula 1) were calculated to assess the flotation effect:

https://doi.org/10.1021/acsomega.4c00572
ACS Omega 2024, 9, 21071−21081

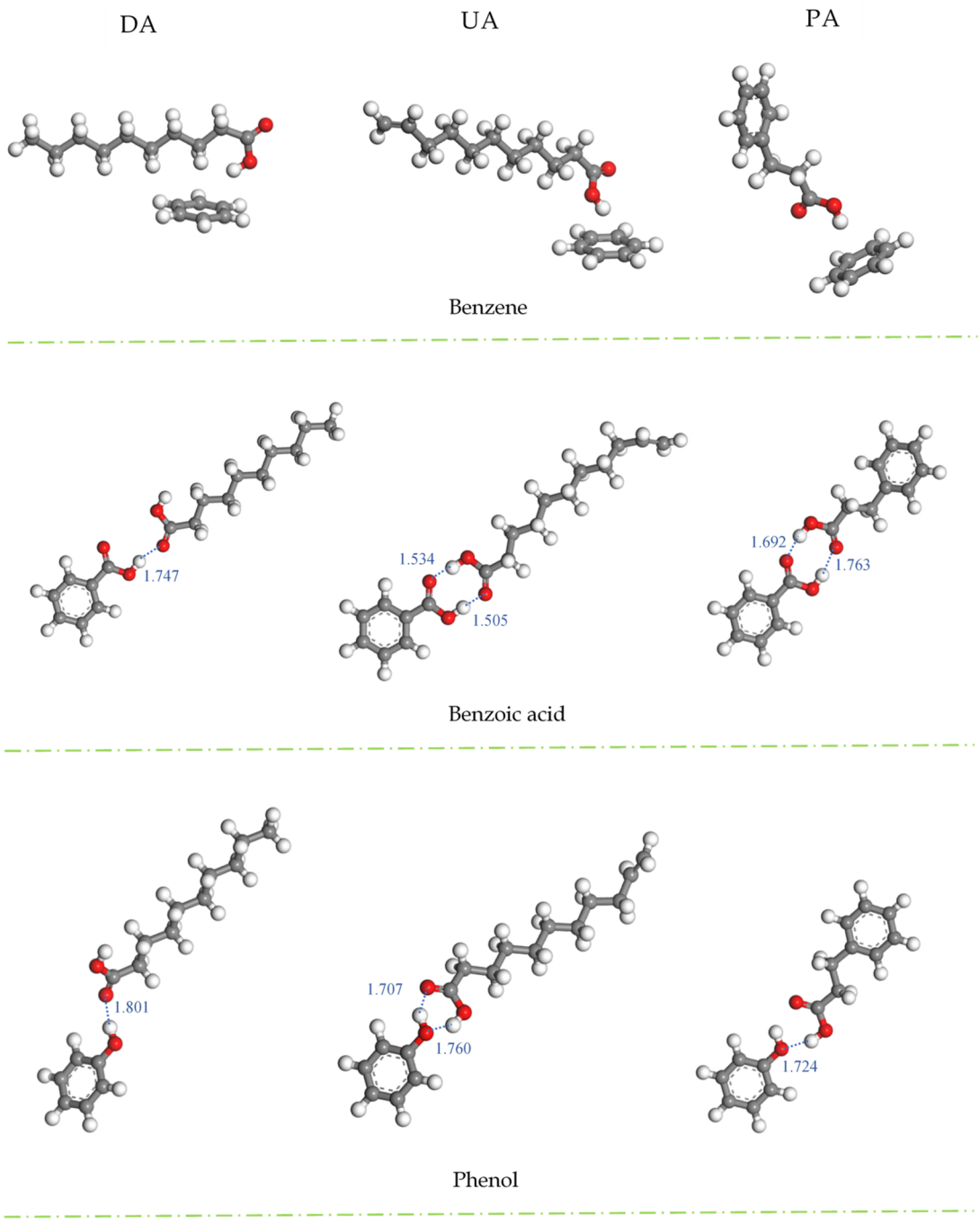

Figure 3. Adsorption configuration of fatty acid molecules with different saturations and low-rank coal molecular fragments.

$$\text{Combustible matter recovery (\%)} = \left(\frac{M_C(100 - A_C)}{M_F(100 - A_F)}\right) \times 100 \quad (1)$$

In the formula, A represents the ash content, M represents the weight, and F and C respectively represent the flotation of cleaned coal and feed.

3. RESULTS AND DISCUSSION

3.1. DFT Calculation of Mixed Collector of Fatty Acids with Different Saturations and LRC/water. Considering the liquid phase environment in the actual flotation, this study predicts the interaction between fatty acid molecules with LRC molecules and water molecules with different saturations based on DFT calculations. Through hydrogen bond distance and Mulliken charge transfer, the recognition phenomenon of different fatty acid molecules on the LRC surface and between them and water molecules is predicted. Furthermore, the interaction strengths of different fatty acid molecules on LRC and water molecules is investigated.

3.1.1. Hydrogen Bond Interactions. The influence of the interaction between mixed collector molecules and water molecules or LRC on the overall interaction strength cannot be ignored. In this investigation, the presence of hydrogen bonding is determined by geometric criteria: hydrogen atoms and acceptor atoms can establish hydrogen bonds at a maximum distance of 2.5 Å, and the acceptor, hydrogen, and donor atoms

https://doi.org/10.1021/acsomega.4c00572
ACS Omega 2024, 9, 21071−21081

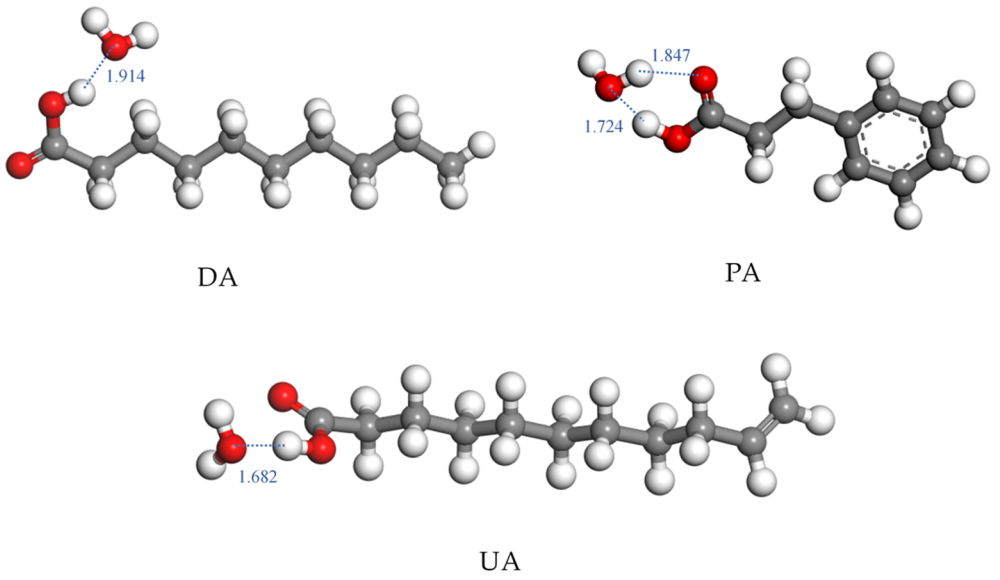

Figure 4. Adsorption configuration of fatty acid molecules with different saturations and water molecules.

Table 1. Change of Atomic Mulliken Charge before and after the Interaction between Fatty Acid Molecules with Different Saturations and Benzene Ring

Molecular name	Atom position		*s*	*p*	Total	Charge (e)
DA-Benzene	H(−COOH)	before	0.47	0	0.47	0.53
		after	0.47	0	0.47	0.53
	O(−C═O)	before	1.83	4.72	6.55	−0.55
		after	1.82	4.74	6.56	−0.56
	O(−OH)	before	1.82	4.85	6.67	−0.67
		after	1.81	4.84	6.65	−0.65
UA-Benzene	H(−COOH)	before	0.45	0	0.45	0.55
		after	0.46	0	0.46	0.54
	O(−C═O)	before	1.83	4.73	6.57	−0.57
		after	1.82	4.75	6.57	−0.57
	O(−OH)	before	1.83	4.87	6.7	−0.7
		after	1.81	4.86	6.66	−0.66
PA-Benzene	H(−COOH)	before	0.45	0	0.45	0.55
		after	0.45	0	0.45	0.55
	O(−C═O)	before	1.83	4.73	6.56	−0.56
		after	1.82	4.75	6.57	−0.57
	O(−OH)	before	1.83	4.88	6.71	−0.71
		after	1.82	4.86	6.67	−0.67

form a hydrogen bond with a minimum angle of 135°.[39] The interaction configuration diagrams of fatty acid molecules with different saturations with LRC molecular fragments and with water molecules are shown in Figure 3 and Figure 4, in which hydrogen bonds that may form between molecules are marked. As can be seen from Figure 3, fatty acid molecules (DA, UA, PA) with different saturations in the mixed collector have the potential to form hydrogen bonds with LRC molecular fragments, benzoic acid, and phenol. Among them, the DA molecule's carbon chain is free of saturated bonds, the carbon−carbon double bond is the unsaturated bond in the UA molecule's carbon chain, and the carbon−carbon link between the single bond and the double bond on the benzene ring is the unsaturated bond in the PA molecule's carbon chain. The benzene ring inclines DA and UA molecules to a certain extent, and the incline degree between the benzene ring and PA molecule is relatively large and almost vertical. In addition, compared with the DA molecule, UA and PA molecules with unsaturated bonds in the carbon chain are mainly carboxyl groups toward the benzene ring. For benzoic acid and phenol, the hydrogen bond strength formed by fatty acid molecules with different unsaturated bond carbon chains with benzoic acid is greater than that formed by phenol. For fatty acid molecules, UA molecules with carbon−carbon double bonds in the carbon chain are most capable of forming hydrogen bonds with benzoic acid/phenol coal molecular fragments and can establish two hydrogen bonds with benzoic acid/phenol molecules, in which the two oxygen atoms on the carboxyl group of UA, oxygen atoms with a single bond acting as a proton donor and one with a double bond acting as a proton acceptor. Only two hydrogen bonds can be formed between PA molecules and benzoic acid. However, the carboxyl group on DA only has the oxygen atom on the double bond as the acceptor to form hydrogen bonds, and the hydrogen bonds formed are all weaker than the other two carboxylic acid molecules. On the whole, the intensity of hydrogen bonding between fatty acid molecules with different

https://doi.org/10.1021/acsomega.4c00572
ACS Omega 2024, 9, 21071−21081

Table 2. Change of Atomic Mulliken Charge before and after the Interaction between Fatty Acid Molecules with Different Saturations and Benzoic Acid

Molecular name	Atom position		*s*	*p*	Total	Charge (e)
DA-Benzoic acid	H (Benzoic acid-COOH)	before	0.45	0	0.45	0.55
		after	0.48	0	0.48	0.52
	O (DA-C═O)	before	1.83	4.72	6.55	−0.55
		after	1.81	4.75	6.56	−0.56
UA-Benzoic acid	H (Benzoic acid-COOH)	before	0.45	0	0.45	0.55
		after	0.51	0	0.51	0.49
	O (UA-C═O)	before	1.83	4.73	6.57	−0.57
		after	1.81	4.78	6.58	−0.58
	H (UA-COOH)	before	0.45	0	0.45	0.55
		after	0.51	0	0.51	0.49
	O (Benzoic acid-C═O)	before	1.83	4.73	6.56	−0.56
		after	1.81	4.77	6.58	−0.58
PA-Benzoic acid	H (Benzoic acid-COOH)	before	0.45	0	0.45	0.55
		after	0.47	0	0.47	0.53
	O (PA-C═O)	before	1.83	4.73	6.56	−0.56
		after	1.8	4.77	6.57	−0.57
	H (PA-COOH)	before	0.45	0	0.45	0.55
		after	0.47	0	0.47	0.53
	O (Benzoic acid-C═O)	before	1.83	4.73	6.56	−0.56
		after	1.8	4.78	6.58	−0.58

Table 3. Change of Atomic Mulliken Charge before and after the Interaction between Fatty Acid Molecules with Different Saturations and Phenol

Molecular name	Atom position		*s*	*p*	Total	Charge (e)
DA-Phenol	H (Phenol-OH)	before	0.46	0	0.46	0.54
		after	0.48	0	0.48	0.52
	O (DA-C═O)	before	1.83	4.72	6.55	−0.55
		after	1.81	4.74	6.55	−0.55
PA-Phenol	H (PA-COOH)	before	0.45	0	0.45	0.55
		after	0.49	0	0.49	0.51
	O (Phenol-OH)	before	1.82	4.89	6.71	−0.71
		after	1.79	4.91	6.7	−0.7
UA-Phenol	H (Phenol-OH)	before	0.46	0	0.46	0.54
		after	0.51	0	0.51	0.49
	O (UA-C═O)	before	1.83	4.74	6.57	−0.57
		after	1.82	4.76	6.58	−0.58
	H (UA-COOH)	before	0.45	0	0.45	0.55
		after	0.49	0	0.49	0.51
	O (Phenol-OH)	before	1.82	4.89	6.71	−0.71
		after	1.8	4.88	6.68	−0.68

unsaturated bonds and coal molecular fragments is UA > PA > DA. The above results indicate that UA molecules with unsaturated carbon−carbon double bonds are more easily adsorbed on LRC molecules through strong hydrogen bonding under the condition of only mixed collectors and LRC. However, the liquid phase water environment needs to be considered in the actual flotation process.

Figure 4 shows the interaction configuration between fatty acid molecules with different saturations and water molecules. Different from the interaction between LRC molecules, PA has the strongest ability to form hydrogen bonds with water molecules and may simultaneously form two hydrogen bonds. Moreover, each hydrogen bond has a greater strength than that of the DA with water molecules. The UA molecule can only form a hydrogen bond with water, but the hydrogen bond formed alone is the strongest. In summary, the results show that UA and PA fatty acid molecules with unsaturated carbon chains can establish strong hydrogen bonds with LRC and water molecules, and DA molecules with saturated carbon chains can form the weakest hydrogen bonds with LRC and water molecules. However, as a result of the directionality and saturation of hydrogen bonding, the capacity of fatty acid molecules with unsaturated bond carbon chains to adhere to the surface of LRC under liquid phase conditions needs to be further discussed and verified in the following part.

3.1.2. Electrostatic Interactions. According to the analysis in section 3.1.1, the changes of Mulliken atom charges before and after the hydrogen bond formation are further calculated, and the changes of hydrogen and oxygen atom charges on carboxyl groups when fatty acid molecules with different unsaturated bond carbon chains interact with benzene rings are also calculated so as to determine the positions where the interaction is more likely to occur. Table 1, Table 2, Table 3, and Table 4 show the changes of atomic charge before and after the

https://doi.org/10.1021/acsomega.4c00572
ACS Omega 2024, 9, 21071−21081

Table 4. Change of Atomic Mulliken Charge before and after the Interaction between Fatty Acid Molecules with Different Saturations and Water Molecules

Molecular name	Atom position		*s*	*p*	Total	Charge (e)
DA−water	H (DA-COOH)	before	0.47	0	0.47	0.53
		after	0.49	0	0.49	0.51
	O (Water-O)	before	1.89	5.16	7.05	−1.05
		after	1.88	5.15	7.03	−1.03
UA−water	H (UA-COOH)	before	0.45	0	0.45	0.55
		after	0.51	0	0.51	0.49
	O (Water-O)	before	1.89	5.16	7.05	−1.05
		after	1.87	5.09	6.96	−0.96
PA−water	H (PA-COOH)	before	0.45	0	0.45	0.55
		after	0.5	0	0.5	0.5
	O (Water-O)	before	1.89	5.16	7.05	−1.05
		after	1.87	5.13	7	−1
	H (Water-H)	before	0.47	0	0.47	0.53
		after	0.5	0	0.5	0.5
	O (PA-C═O)	before	1.83	4.73	6.56	−0.56
		after	1.82	4.76	6.58	−0.58

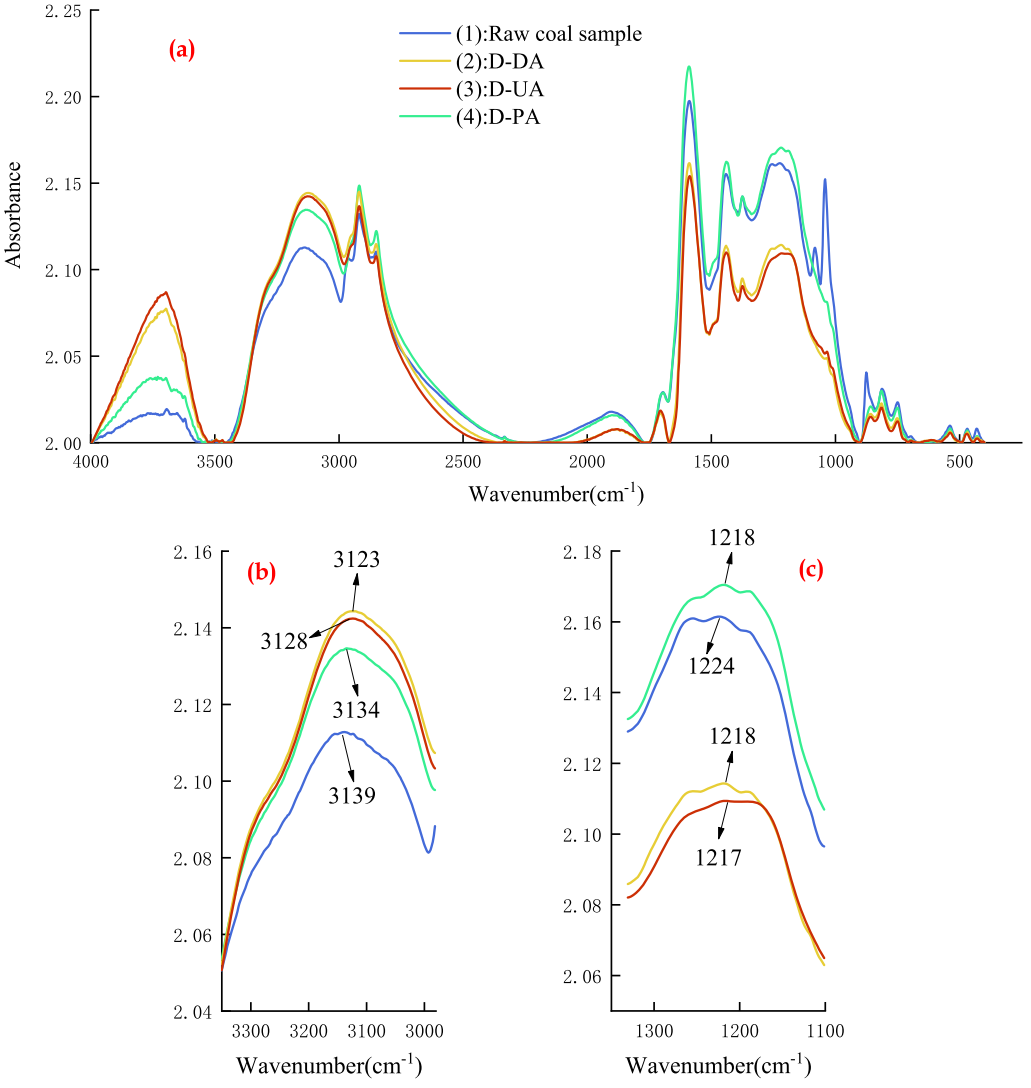

Figure 5. (a) FTIR spectra of mixed collectors with different saturated fatty acids before and after adsorption with low-rank coal. (b) Amplifying spectral peak diagram of (a) ranging from 2980 to 3350 cm^{-1}. (c) Amplifying spectral peak diagram of (a) ranging from 1140 to 1330 cm^{-1}.

interaction of fatty acid molecules with different unsaturated bond carbon chains with the benzene ring, benzoic acid, phenol, and water molecules. As can be seen from Table 1, for benzene rings formed without hydrogen bonding, when fatty acid

https://doi.org/10.1021/acsomega.4c00572
ACS Omega 2024, 9, 21071−21081

molecules have various unsaturated bond carbon chains, there is relatively little hydrogen atom charge transfer between the carboxyl groups on those molecules. When the fatty acid molecule's carbon chain has unsaturated bonds, the O atom (−OH) on the carboxyl group loses charge gradually, and the O atom (−OH) in UA and PA molecules both lose 0.04e, while the H atom (−COOH) and another O atom (−C═O) on the fatty acid molecule have almost no charge transfer. In conclusion, the interaction between the benzene ring and fatty acid molecules is mainly intermolecular force, but the interaction is weak, and the carbon chain containing unsaturated bonds will enhance the interaction between the benzene ring and carboxyl group in fatty acid molecules.

Comparing the three tables from Table 2 to Table 4, it can be observed that the same atom (−C═O) on the fatty acid molecule acts as the acceptor in hydrogen bonding with benzoic acid and phenol, and the charge transfer is rarely 0.01e or even no charge transfer, indicating that the oxygen of the carbon−oxygen double bond on the fatty acid molecule is relatively stable and is not affected by the unsaturated bond in the carbon chain. For the H atom in hydrogen bonding, when the H atom is the hydrogen atom in the polar functional group of benzoic acid/phenol in the carboxylic acid molecular-benzoic acid/phenol interaction system, the 1s orbital of the H atom (benzoic acid-COOH/phenol-OH) is 0.06e when the UA molecule interacts with benzoic acid/phenol, showing the most active performance. As another hydrogen bond H atom (UA-COOH) forms a hydrogen bond with benzoic acid/phenol, it can get 0.06e and 0.04e, respectively, which is also active enough. For DA and PA molecules, the H atom (benzoic acid-COOH) gets 0.03e and 0.02e, respectively, but when forming a hydrogen bond with phenol, the H atom forming a hydrogen bond with the DA molecule is phenol-OH, which gets 0.02e, while the H atom in the hydrogen bond formed by the PA molecule and phenol is provided by PA-COOH, which gets 0.04e. This is consistent with the strength of hydrogen bonding UA > PA > DA between carbon chain fatty acid molecules with different unsaturated bonds and coal molecular fragments separately in the above section.

For the fatty acid−water interaction system, the H atom in hydrogen bonding is mainly provided by the hydrogen atom in the fatty acid molecule, and the acceptant O atom is an oxygen atom in the water molecule, in which the H atom (−COOH) on DA, UA, and PA gets 0.02e, 0.06e, and 0.05e, respectively. The O atom of the acceptor interacting with DA, UA, and PA molecules lost 0.02e, 0.09e, and 0.05e, respectively. In addition, the H atom and the O atom in another hydrogen bond between PA and water molecule gain and lose 0.02e, respectively. The individual charge transfer amount of UA molecules interacting with water is greater than that of UA molecules interacting with benzoic acid/phenol, but only one hydrogen bond is formed. The single charge transfer amount of PA molecules interacting with water molecules is larger than that of PA molecules interacting with benzoic acid and phenol, and it can form two hydrogen bonds with water molecules. Therefore, the comprehensive analysis of hydrogen bond results shows that the hydrogen bond between fatty acid molecules UA and PA with unsaturated bonded carbon chains and benzoic acid/phenol/water molecules is stronger than that between DA molecules without unsaturated bonded carbon chains, and the electrostatic interaction between them is also the strongest (no matter whether LRC molecules or water molecules). In addition, the interactions between the molecules of UA and water are greater than those between UA and phenol, and the interactions between the molecules of PA and water are stronger than those between PA and the fragment of the LRC (benzene/benzoic acid/phenol), indicating that the fatty acid molecule with unsaturated bond carbon chain strengthens the interaction with water molecule on the whole, and even PA molecule preferentially interacts with water molecule. It is unfavorable for the mixed collector to act on the LRC flotation.

3.2. FTIR Analysis. Figure 5 displays the FTIR spectra of the mixed collector before and after adsorption with different unsaturated bond carbon chains and LRC. The amplified spectral peaks of Figure 5(a) are depicted in Figure 5(b),(c), respectively, with wave numbers between 2980 and 3350 cm^{-1} and between 1140 and 1330 cm^{-1}. The main groups corresponding to the two magnification ranges are as follows: the absorption peak at 3400−3100 cm^{-1} represents the stretching vibration peak of the hydroxyl group forming the intermolecular hydrogen bond (−OH), and the absorption peak at 1140−1250 cm^{-1} represents the stretching vibration peak of the alkane carbon−carbon single bond (C−C).[40,41] Because of the intermolecular hydrogen bonds formed during the mixed collector's process of adhering to the LRC surface, the hydrogen bond effect will reduce the stretching vibration frequency of the hydroxyl group, so that the absorption peak of the −OH moves to the low-frequency direction.[42,43] In other words, when moving in the direction of a lower wavenumber, the greater the hydrogen bonding intensity, the greater the distance of the absorption peak. As shown in Figure 5(a), (1)−(4) are the LRC original samples, and the samples are adsorbed by the mixed collector (D-DA, D-UA, D-PA) of a carbon chain with different saturations, respectively. The characteristic peaks of 3139, 3123, 3128, and 3134 cm^{-1} are, respectively, the stretching vibration peaks of hydroxyl groups forming intermolecular hydrogen bonds in samples (1)−(4). Compared with the characteristic peaks of the original samples of LRC, the travel distances of characteristic peaks of coal samples treated with mixed collectors are 16, 11, and 5 cm^{-1}, respectively, indicating that the hydrogen bonding strength between mixed collectors with different unsaturated bond carbon chains and LRC is D-DA > D-UA > D-PA. According to the DFT calculation results, the interaction between PA molecules and water molecules was stronger than that between PA molecules and LRC molecular fragments. It shows that in the liquid phase environment, taking into account the powerful hydrogen bonds that exist between water molecules and unsaturated carbon chain fatty acid molecules, it will indirectly weaken the strength of hydrogen bonding between PA and LRC molecules, resulting in the shortest travel distance of the hydroxyl characteristic peak in LRC samples treated with D-PA. Stronger interactions between UA molecules and water molecules than UA molecules with phenol are seen, so the movement distance of the D-UA characteristic peak is moderate. The interaction between DA molecules and LRC and water molecules is similar, so the D-DA characteristic peak moves the longest distance. In addition, Figure 5(c) shows that the characteristic peaks of C−C in spectra (1)−(4) are 1224, 1218, 1217, and 1218 cm^{-1}. Following adsorption by the mixed collector with different saturated fatty acids, the C−C migration distance of the LRC samples is close. Compared with the unsaturated bond type, the carbon chain length seems to have a greater influence on the adsorption of the LRC hydrophobic points.

3.3. Zeta Analysis. In the liquid phase, the existence of polar oxygen-containing groups such as −COOH and −OH is directly

https://doi.org/10.1021/acsomega.4c00572
ACS Omega 2024, 9, 21071−21081

related to the electric potential of LRC particles. When the coal particles are dispersed, these groups can be protonated or ionized, resulting in the overall negative electric potential of LRC (−7.42 mv).[44,45] Figure 6 demonstrates that when coal

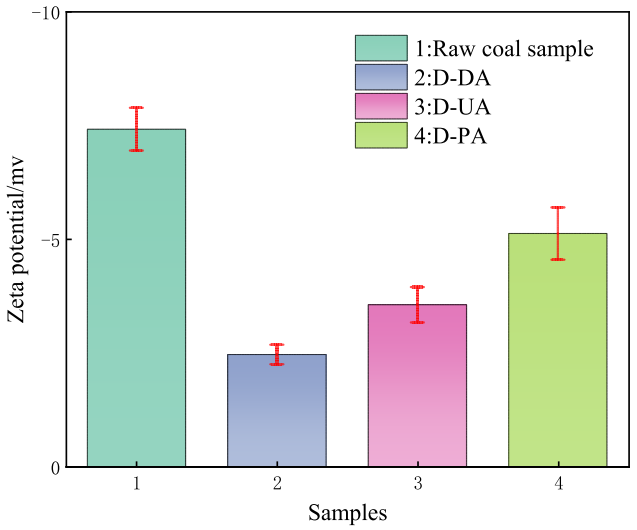

Figure 6. Zeta potential of the coal samples treated with mixed collectors with different saturated fatty acids.

samples are treated with mixed collectors with different saturated fatty acids, the absolute value of the Zeta potential clearly falls. It shows that agglomeration occurs between the coal particles and the reagent, resulting in changes in the electric potential of the coal surface. For the mixed collector, the coal samples treated with D-DA without a saturated bond carbon chain have the smallest absolute value of the Zeta potential, and the potential value is −2.45mv; that is, the surface potential change range of LRC particles is the largest, then D-UA (−3.55mv), and finally D-PA (−5.12mv). According to the FTIR analysis results in the above section, the hydrogen bonding between DA molecules without saturated bond carbon chains and water molecules is the weakest in the liquid phase environment; therefore, DA molecules can be adsorbed to oxygen-containing functional groups like −COOH and −OH on the surface of LRC particles through hydrogen bonding. Since the strongest hydrogen bond exists between the molecules of PA and water, the hydrogen bond interaction of D-PA with the LRC surface is prevented. Consequently, the adsorption of D-PA on coal particle surfaces is the weakest, and the change range of the Zeta potential is the smallest.

3.4. Flotation Results. Figure 7 shows the flotation results of pure coal samples by a mixed collector with different saturated fatty acids. For the D-DA without a saturated bond carbon chain, the flotation clean coal yield has reached 95.21% at a dosage of 2 kg/t, and nearly all useful minerals have been floated. The yield of flotation clean coal rises only modestly with an increase in reagent dosage. For the D-UA, with a carbon−carbon double bond, the flotation clean coal yield is 88.04% when the dosage is 2 kg/t, and it can reach 96.90% when the dosage is 3 kg/t. For the D-PA with a benzene ring, the flotation clean coal yield is 85.71% at a dose of 3 kg/t, far lower than that obtained by the other two mixed collectors at the same dosage. The flotation clean coal yield can reach 94.17% at a dosage of 4 kg/t, and then the yield increases slightly. The results show that the flotation clean coal yield obtained by using a nonsaturated bond carbon

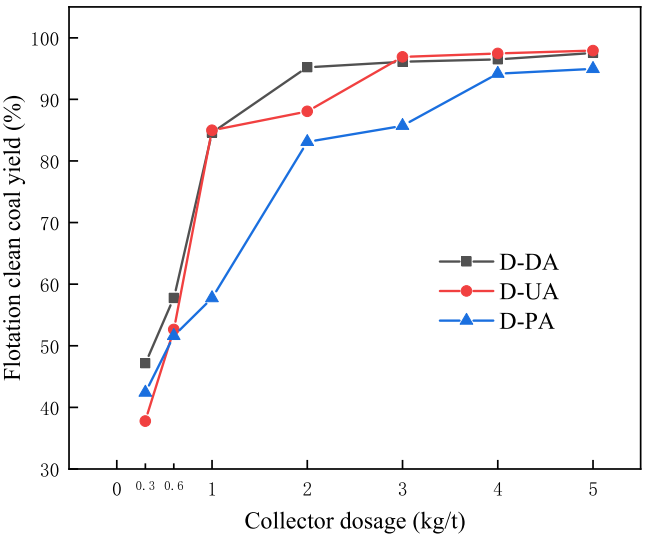

Figure 7. Flotation results of mixed collectors with different saturated fatty acids on pure coal samples.

chain is the highest, followed by D-UA and D-PA at the lower dosage level. This indicates that in the actual flotation process, the strong hydrogen bonding between UA and PA and water as well as the electrostatic interaction weakens the collection performance of the mixed collectors D-UA and D-PA for LRC.

In the pure coal flotation experiment, when the amount of collector reagent is greater than 2 kg/t, a higher cleaned coal yield can be obtained, and the yield rises relatively slowly as the reagent amounts are increased. Therefore, in the actual coal sample flotation experiments, the dosage of the mixed collector is fixed at 3 kg/t, and their flotation behavior on the actual coal sample of the LRC is investigated. Figure 8 shows the flotation

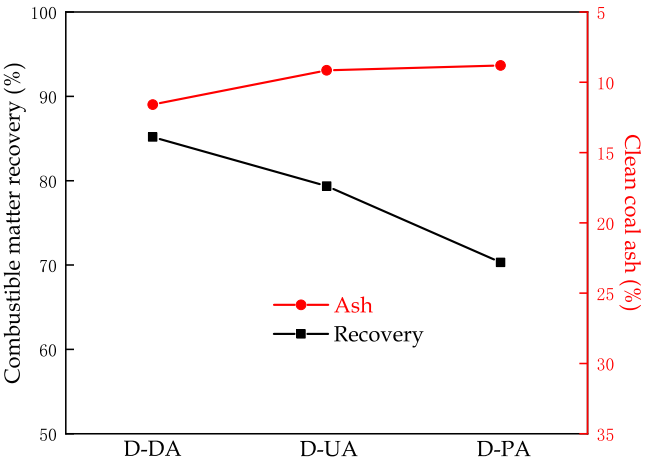

Figure 8. Flotation results of mixed collectors with different saturated fatty acids on actual coal samples.

results of actual coal samples. The bottom half of the figure is divided into the combustible matter recovery obtained from the actual coal sample flotation, and the top half is the corresponding cleaned coal ash. From Figure 8, it is clear that the combustible matter recovery is obtained in the order from large to small, D-DA (85.18%) > D-UA (79.35%) > D-PA (70.32%), and the cleaned coal ash from large to small order is D-DA (11.59%) > D-UA (9.15%) > D-PA (8.80%). The cleaned coal ash difference is not much. Both results meet the

https://doi.org/10.1021/acsomega.4c00572
ACS Omega 2024, 9, 21071−21081

requirements of flotation clean coal ash. The highest combustible matter recovery is obtained utilizing D-DA under the same flotation conditions, followed by D-UA, and D-PA is the lowest. In conclusion, D-DA > D-UA > D-PA is the sequence in which mixed collectors with various saturated fatty acids have an impact on LRC flotation, which agrees with the above research results.

4. CONCLUSIONS

(1) The DFT analysis's findings revealed that the hydrogen bonding between fatty acid molecules UA/PA with unsaturated bonds and benzoic acid/phenol/water molecules was stronger than DA molecules without unsaturated bonds, and the electrostatic interaction between the two molecules was also the strongest (whether it was an LRC fragment or water molecule). The interaction between UA and water molecules was stronger than that between UA and phenol, and the interaction between PA molecules and water molecules was stronger than that between PA molecules and LRC molecular fragments (benzene/benzoic acid/phenol), indicating that fatty acid molecules containing unsaturated bonds strengthened the interaction with water molecules as a whole. Even PA molecules would preferentially adsorb water molecules, which was unfavorable to the effect of mixed collectors on LRC flotation.

(2) According to the findings of FTIR and Zeta potential, the adsorption of LRC at the hydrophobic site was not significantly affected by the unsaturated bond, mostly as a result of the effect of carbon chain length, and the hydrogen bond strength between the mixed collector with different saturation fatty acids and LRC is D-DA > D-UA > D-PA.

(3) The flotation experiments of pure coal and actual coal samples showed that the order of the flotation effect of mixed collectors with different saturations on LRC is D-DA > D-UA > D-PA, indicating that in the actual flotation process, the strong electrostatic interaction and the hydrogen bond between UA/PA and water weaken the collection performance of the mixed collector D-UA/D-PA for LRC, which also confirmed the research results of DFT, FTIR, and Zeta.

AUTHOR INFORMATION

Corresponding Authors

Zechen Liu − *School of Mining Engineering, Taiyuan University of Technology, Taiyuan 030024 Shanxi, PR China; Chinese National Engineering Research Center of Coal Preparation and Purification, China University of Mining and Technology, Xuzhou 221116 Jiangsu, PR China;* orcid.org/0000-0002-9117-0528; Phone: +86 18334705768; Email: liuzechen1995@126.com

Xianshu Dong − *School of Mining Engineering, Taiyuan University of Technology, Taiyuan 030024 Shanxi, PR China;* Phone: +86 13099093565; Email: dongxianshu@tyut.edu.cn

Authors

Yinfei Liao − *Chinese National Engineering Research Center of Coal Preparation and Purification, China University of Mining and Technology, Xuzhou 221116 Jiangsu, PR China;* orcid.org/0000-0003-1729-7288

Yuping Fan − *School of Mining Engineering, Taiyuan University of Technology, Taiyuan 030024 Shanxi, PR China*

Yijun Cao − *Chinese National Engineering Research Center of Coal Preparation and Purification, China University of Mining and Technology, Xuzhou 221116 Jiangsu, PR China; Zhongyuan Critical Metals Laboratory, Zhengzhou University, Zhengzhou 450001, PR China;* orcid.org/0000-0002-4635-0829

Complete contact information is available at: https://pubs.acs.org/10.1021/acsomega.4c00572

Notes

The authors declare no competing financial interest.

ACKNOWLEDGMENTS

This research was financially supported by the National Natural Science Foundation of China (Grant Nos. 52304292, 51820105006) and Fundamental Research Program of Shanxi Province (Grant Nos. 202303021212048). Computation time and software resources were provided by the National Supercomputing Center in Shenzhen, P. R. China. At the same time, the authors would like to thank the Shanxi Supercomputing Center of China for its technical support in simulation calculations.

REFERENCES

(1) Liu, J.; Zhang, R.; Bao, X.; Hao, Y.; Gui, X.; Xing, Y. New insight into the role of the emulsified diesel droplet size in low rank coal flotation. *Fuel* **2023**, *338*, 127388.

(2) Saha, B.; Patra, A. S.; Das, A.; Basu, A.; Mukherjee, A. K. Role of collector polarity and size on the low-rank fine coal flotation. *Int. J. Coal Prep Util* **2023**, *43*, 203−216.

(3) Zhao, D.; Liu, X. Effect of ionic surfactants on flotation of low-rank coal: a DFT calculation and MD simulation study. *Mol. Phys.* **2022**, *120*, 120.

(4) Wang, P.; Liu, W.; Zhuo, Q.; Luo, Q.; Sun, X.; Li, J. Mechanism of interaction between mixed collectors and low-rank coal: An experimental and simulation study. *Int. J. Coal Prep Util* **2023**, *43*, 346−360.

(5) Du, R.; Tuo, B.; Wang, J.; Gu, D.; Nie, G.; Tang, Y. Synergistic effect of SPS compound surfactant and diesel oil on low-rank coal slime flotation. *Int. J. Coal Prep Util* **2023**, *43*, 2091.

(6) Zhang, L.; Sun, X.; Li, B.; Xie, Z.; Guo, J.; Liu, S. Experimental and molecular dynamics simulation study on the enhancement of low rank coal flotation by mixed collector. *Fuel* **2020**, *266*, 117046.

(7) Filippova, I. V.; Filippov, L. O.; Duverger, A.; Severov, V. V. Synergetic effect of a mixture of anionic and nonionic reagents: Ca mineral contrast separation by flotation at neutral pH. *Miner Eng.* **2014**, *66*, 135−144.

(8) Gui, X.; Xing, Y.; Wang, T.; Cao, Y.; Miao, Z.; Xu, M. Intensification mechanism of oxidized coal flotation by using oxygen-containing collector α-furanacrylic acid. *Powder Technol.* **2017**, *305*, 109−116.

(9) Lyu, X.; You, X.; He, M.; Zhang, W.; Wei, H.; Li, L.; et al. Adsorption and molecular dynamics simulations of nonionic surfactant on the low rank coal surface. *Fuel* **2018**, *211*, 529−534.

(10) Liu, Z.; Xia, Y.; Lai, Q.; An, M.; Liao, Y.; Wang, Y. Adsorption behavior of mixed dodecane/n-valeric acid collectors on low-rank coal surface: Experimental and molecular dynamics simulation study. *Colloids Surfaces A Physicochem Eng. Asp* **2019**, *583*, 123840.

(11) Li, M.; Xia, Y.; Zhang, Y.; Ding, S.; Rong, G.; Cao, Y.; et al. Mechanism of shale oil as an effective collector for oxidized coal flotation: From bubble−particle attachment and detachment point of view. *Fuel* **2019**, *255*, 115885.

(12) Liao, Y.; Ren, H.; An, M.; Cao, Y.; Ma, L.; Hao, X.; et al. Kinetics of bubble interaction with low rank coal surface in the presence of adsorbed dodecane-oleic acid collector mixture. *Int. J. Coal Prep Util* **2022**, *42*, 2756.
(13) Guo, W.; Cai, Y.; Zhu, Y.; Li, Y.; Sun, Y. Comparative Studies on Flotation Performance of Saturated Fatty Acids and Unsaturated Fatty Acids Separated from Hogwash Oil. *Minerals* **2021**, *11*, 50.
(14) Yu, H.; Wang, H.; Sun, C. Comparative studies on phosphate ore flotation collectors prepared by hogwash oil from different regions. *Int. J. Min Sci. Technol.* **2018**, *28*, 453−459.
(15) Yuehua, H. U.; Haisheng, H. A. N.; Mengjie, T.; Wei, S. U. N.; Jianjun, W.; Zhao, W. E. I.; et al. The Application of Metal − coordinated Complexes in the Flotation of Oxide Minerals and Fundamental Research of the Adsorption Mechanism. *Conservation and Utilization of Mineral Resources* **2018**, 42.
(16) Sun, W.; Wang, J.; Han, H.; Wang, L.; Liu, R.; Sun, W. Advances in flotation reagent interfacial assembly technology. *Zhongguo Kuangye Daxue Xuebao/Journal China Univ Min Technol.* **2022**, *51*, 544−553.
(17) Cui, W.; Zhang, J.; Chen, J. Surface proximity effect of galena and its influence on synergistic adsorption behavior. *Appl. Surf. Sci.* **2021**, *567*, 150847.
(18) Sun, R.; Ge, J.; Yao, J.; Li, S.; Shen, H.; Gu, R. Predicting the binding capability of benzothiazoline-2-thione and its derivatives with gold: A DFT and FT-Raman combined studies. *Spectrochim Acta - Part A Mol. Biomol Spectrosc* **2008**, *71*, 1535−1539.
(19) Zhao, G.; Zhong, H.; Qiu, X.; Wang, S.; Gao, Y.; Dai, Z.; et al. The DFT study of cyclohexyl hydroxamic acid as a collector in scheelite flotation. *Miner Eng.* **2013**, *49*, 54−60.
(20) Choudhary, N.; Bee, S.; Gupta, A.; Tandon, P. Comparative vibrational spectroscopic studies, HOMO-LUMO and NBO analysis of N-(phenyl)-2,2-dichloroacetamide, N-(2-chloro phenyl)-2,2-dichloroacetamide and N-(4-chloro phenyl)-2,2-dichloroacetamide based on density functional theory. *Comput. Theor Chem.* **2013**, *1016*, 8−21.
(21) Mahmoudi, O.; Bordjiba, T.; Affoune, A. M. Density functional theory study of the interaction of 2-mercaptobenzimidazole and gold, palladium and nickel atoms. *Int. J. Electrochem Sci.* **2016**, *11*, 4427−4441.
(22) Moss, C. L.; Isborn, C. M.; Li, X. Ehrenfest dynamics with a time-dependent density-functional-theory calculation of lifetimes and resonant widths of charge-transfer states of Li+ near an aluminum cluster surface. *Phys. Rev. A* **2009**, *80*, 024503.
(23) Liu, J.; Wen, S.; Deng, J.; Chen, X.; Feng, Q. DFT study of ethyl xanthate interaction with sphalerite (1 1 0) surface in the absence and presence of copper. *Appl. Surf. Sci.* **2014**, *311*, 258−263.
(24) Li, B.; Liu, S.; Guo, J.; Zhang, L.; Sun, X. Increase in wettability difference between organic and mineral matter to promote low-rank coal flotation by using ultrasonic treatment. *Appl. Surf. Sci.* **2019**, *481*, 454−459.
(25) Zou, W.; Yu, C.; Sun, C.; Cao, Y. Selective adsorption of anionic polyacrylamide onto ultra-low ash coal and kaolinite. *Physicochem. Probl. Miner. Process.* **2016**, *52*, 738−753.
(26) Liu, Z.; Liao, Y.; Wang, Y.; An, M.; Lai, Q. Enhancing low-rank coal flotation using a mixture of dodecane and n-valeric acid as a collector. *Int. J. Coal Prep Util* **2022**, *42*, 97.
(27) Liu, Z.; Ren, H.; Yang, Z.; Liao, Y.; Wang, Y. Effect of mixing ratio on the adsorption behavior of low-rank coal surface using mixed collectors: Experimental and molecular dynamics simulation study. *Int. J. Coal Prep Util* **2022**, *42*, 2788−2803.
(28) Li, B.; Liu, S.; Guo, J.; Zhang, L. Interaction between low rank coal and kaolinite particles : A DFT simulation. *Appl. Surf. Sci.* **2018**, *456*, 215−220.
(29) Li, B.; Liu, S.; Guo, J.; Zhang, L.; Sun, X. Increase in wettability difference between organic and mineral matter to promote low-rank coal flotation by using ultrasonic treatment. *Appl. Surf. Sci.* **2019**, *481*, 454−459.
(30) Montoya, A.; Mondragón, F.; Truong, T. N. Adsorption on carbonaceous surfaces: Cost-effective computational strategies for quantum chemistry studies of aromatic systems. *Carbon N Y* **2002**, *40*, 1863−1872.
(31) Perdew, J. P.; Burke, K.; Ernzerhof, M. Generalized Gradient Approximation Made Simple. *Phys. Rev. Lett.* **1996**, *77*, 3865.
(32) Carpenter, B.; Gelman, A.; Hoffman, M. D.; Lee, D.; Goodrich, B.; Betancourt, M. Stan : A Probabilistic Programming Language. *J. Stat. Soft.* **2017**, *76*, 76.
(33) Yu, S.; Bo, J.; Wu, L. Molecular simulation of CH4/CO2/H2O competitive adsorption on low rank coal vitrinite. *Phys. Chem. Chem. Phys.* **2017**, *19*, 17773−17788.
(34) Dong, K.; Zeng, F.; Jia, J.; Chen, C.; Gong, Z. Molecular simulation of the preferential adsorption of CH4 and CO2 in middle-rank coal. *Mol. Simul* **2019**, *45*, 15−25.
(35) Bunte, S. W.; Sun, H. Molecular Modeling of Energetic Materials: The Parameterization and Validation of Nitrate Esters in the COMPASS Force Field. *J. Phys. Chem. B* **2000**, *104*, 2477−2489.
(36) Sun, H. The COMPASS force field: Parameterization and validation for phosphazenes. *Comput. Theor. Polym. Sci.* **1998**, *8*, 229−246.
(37) Hampton, M. A.; Nguyen, A. V. Accumulation of dissolved gases at hydrophobic surfaces in water and sodium chloride solutions: Implications for coal flotation. *Miner Eng.* **2009**, *22*, 786−792.
(38) Tian, B.; Qiao, Y.-y.; Tian, Y.-y.; Xie, K.-c.; Liu, Q.; Zhou, H.-f. FTIR study on structural changes of different−rank coals caused by single/multiple extraction with cyclohexanone and NMP/CS2 mixed solvent. *Fuel Process. Technol.* **2016**, *154*, 210−218.
(39) Xu, Y.; Liu, Y. L.; Gao, S.; Jiang, Z. W.; Su, D.; Liu, G. S. Monolayer adsorption of dodecylamine Surfactants at the mica/water interface. *Chem. Eng. Sci.* **2014**, *114*, 58−69.
(40) Çinar, M. Floatability and desulfurization of a low-rank (Turkish) coal by low-temperature heat treatment. *Fuel Process. Technol.* **2009**, *90*, 1300−1304.
(41) Zhu, H.; Li, H.-L.; Ou, Z.-S.; Wang, D.-Z.; et al. Study on Surface Modification of Different Rank Coals by Using FTIR. *J. China Univ Min Technol.* **2001**, *1964*, 366−370.
(42) Wu, Q.; Liu, X.; Berglund, L. A. FT-IR spectroscopic study of hydrogen bonding in PA6/clay nanocomposites. *Polymer* **2002**, *43*, 2445−2449.
(43) Holland, B. J.; Hay, J. N. The dependence of non-volatile residue formation in nylon 6 and nylon 6,6 during thermal degradation on hydrogen bonding in the melt. *Polymer* **2001**, *42*, 4759−4761.
(44) Chen, S.; Wang, S.; Li, L.; Qu, J.; Tao, X.; He, H. Exploration on the mechanism of enhancing low-rank coal flotation with cationic surfactant in the presence of oily collector. *Fuel* **2018**, *227*, 190−198.
(45) Milanović, L.; Posch, H. A.; Hoover, W. G. What is 'liquid'? Understanding the states of matter. *Mol. Phys.* **1998**, *95*, 281−287.

https://doi.org/10.1021/acsomega.4c00572
ACS Omega 2024, 9, 21071−21081